Published in final edited form as:
Nanomedicine (Lond). 2014 February ; 9(2): 237–251. doi:10.2217/nnm.13.58.

Gold nanoparticle–M2e conjugate coformulated with CpG induces protective immunity against influenza A virus

Wenqian Tao[1], **Katherine S Ziemer**[2], and **Harvinder S Gill**[*,1]

[1]Department of Chemical Engineering, Texas Tech University, Lubbock, TX 79409, USA

[2]Department of Chemical Engineering, Northeastern University, Boston, MA 02115, USA

Abstract

Aim: This study aimed to develop a novel influenza A vaccine by conjugating the highly conserved extracellular region of the matrix 2 protein (M2e) of influenza A virus to gold nanoparticles (AuNPs) and to test the vaccine in a mouse influenza challenge model.

Materials & methods: Citrate-reduced AuNPs (diameter: 12 nm) were synthesized, and characterized by transmission electron microscopy and dynamic light scattering. M2e was conjugated to AuNPs through thiol–gold interactions to form M2e–AuNP conjugates. Particle stability was confirmed by UV–visible spectra, and M2e conjugation was further characterized by x-ray photoelectron spectroscopy. Mice were immunized with M2e–AuNPs with or without CpG (cytosine-guanine rich oligonucleotide) as an adjuvant with appropriate control groups. Sera was collected and M2e-specific immunoglobulin (IgG) was measured, and immunized mice were challenged with PR8-H1N1 influenza virus.

Results: M2e-capped AuNPs could be lyophilized and stably resuspended in water. Intranasal vaccination of mice with M2e–AuNP conjugates induced M2e-specific IgG serum antibodies, which significantly increased upon addition of soluble CpG as adjuvant. Upon challenge with lethal PR8, mice vaccinated with M2e-AuNP conjugates were only partially protected, while mice that received soluble CpG as adjuvant in addition to M2e–AuNP were fully protected.

Conclusion: Overall, this study demonstrates the potential of using the M2e–AuNP conjugates with CpG as an adjuvant as a platform for developing an influenza A vaccine.

Keywords

gold nanoparticle; influenza vaccine; influenza virus; M2e; XPS

[*]Author for correspondence: Tel.: +1 806 742 3682 Fax: +1 806 742 3552 harvinder.gill@ttu.edu.

Disclaimer

The content is solely the responsibility of the authors and does not necessarily represent the official views of the NIH.

Financial & competing interests disclosure

W Tao and HS Gill have submitted a provisional patent to the United States Patent and Trademark Office on the use of gold nanoparticles for influenza vaccination through the Texas Tech University System Office of Research, Commercialization & Federal Relations.

The authors have no other relevant affiliations or financial involvement with any organization or entity with a financial interest in or financial conflict with the subject matter or materials discussed in the manuscript apart from those disclosed.

No writing assistance was utilized in the production of this manuscript.

Ethical conduct of research

The authors state that they have obtained appropriate insti tutional review board approval or have followed the princi ples outlined in the Declaration of Helsinki for all human or animal experimental investigations. In addition, for investi gations involving human subjects, informed consent has been obtained from the participants involved.

Influenza, one of the main viral diseases, continues to devastate human lives each year. Influenza virus is contagious and spreads through the respiratory tract, including the nose, throat and bronchi, and can produce pandemics due to its rapid transmission. Three pandemics have already resulted from influenza outbreaks in the 20th century. The first was the 1918 Spanish influenza, which resulted in an estimated 50 million deaths worldwide and is perhaps the most fatal event recorded in human history [1]. The other two influenza pandemics followed in 1957 and 1968, each producing approximately 1 million deaths worldwide [1]. Furthermore, seasonal influenza epidemics result in an estimated 23,607 deaths in the USA [2] and up to 0.5 million deaths worldwide [101].

Influenza A virus expresses two dominant membrane proteins, the hemagglutinin (HA) and neuraminidase (NA). HA allows the virus to infect cells through interaction with sialic acid residues on receptors and NA enables the virus buds to escape from infected cells to spread infection [3]. Current commercial influenza A vaccines use inactivated split influenza viruses as antigens. Neutralizing antibodies against HA are believed to provide the protective immunity. However, owing to mutations in HA and NA, antigenic drift occurs over time in influenza A virus, resulting in new strains of virus that are not recognized by pre-existing antibodies in humans. Consequently, the influenza vaccine has to be modified constantly to follow the antigenic drift of the virus. Less frequently, a major re-assortment in HA and NA genes can occur, resulting in a completely new subtype of influenza A virus that does not naturally circulate in human populations. Such drifts often result in virulent influenza strains that have the potential to cause pandemics. It is, therefore, critical that more universal vaccination strategies are developed against influenza A that can protect against all influenza A subtypes, irrespective of the inherent instability and high mutation rates that exist in the influenza genome.

Unlike HA and NA, the matrix 2 protein (M2) present on influenza virus is a remarkably conserved integral membrane protein of 97 amino acids [4]. The 23-amino acid-long extracellular region of M2 (M2e) is considered one of the most promising antigens for developing an effective universal influenza vaccine. However, a major challenge in developing a vaccine based on M2e is that M2 naturally occurs in very small quantities on virus surfaces (~16–20 molecules per virion) [5,6] and is poorly immunogenic. However, it has been found that by conjugating M2e to appropriate larger antigen carriers, the immunogenicity of the M2e peptide can be significantly improved and M2e-specific immune responses capable of protecting mice against a lethal influenza A challenge can be induced. In the study by Neirynck *et al.*, fusion of M2e to the hepatitis B virus core protein with incomplete Freund's adjuvant provided 90–100% protection against a lethal virus challenge [7]. Other antigen carriers such as keyhole limpet hemocyanin [8], human papilloma virus [9], bacteria [10,11], liposomes [12], virus-like particles [13] and flagellin [14] have been tested. In another strategy, M2e has been developed as a dendrimer containing multiple branched copies of M2e [15,16]. However, many of these studies have used potent yet potentially toxic adjuvants, including derivatives of cholera toxins or heat labile endotoxin, saponin QS21, keyhole limpet hemocyanin and Freund's adjuvant [8,10,17,18]. Thus, there continues to be a strong need for developing alternative and novel vaccine delivery platforms that can present influenza M2e at a high density and can potentially be delivered through the mucosal route, since many studies have demonstrated that intranasal delivery of M2e-based vaccines induces better protection against influenza A virus than the parenteral route [19,20].

Gold nanoparticles (AuNPs) have attracted much research interest in the medical field. Recently, they have also been investigated as antigen carriers [21-26]. The major attractive features of AuNPs as antigen carriers are: the AuNP carrier is inert and does not cause a competing carrier-directed antibody response like other biological carriers, such as hepatitis

B virus core; the size of AuNPs can be easily changed to mimic virions of different types [27,28]; antigens can be presented in high densities on AuNP surfaces to increase their interaction with antigen-presenting cells [29,30]; peptide–AuNP conjugates have been found to be internalized by macrophages resulting in their activation, thus suggesting an adjuvant activity of AuNPs [31]; AuNPs can be produced on a large scale with tight control over nanoparticle sizes [32]; AuNPs can be readily conjugated with peptides by simple mixing with thiol-terminated peptides [33], thus offering a highly flexible and customizable approach to designing AuNP-based vaccines; and AuNP–Peptide conjugates can potentially be lyophilized to produce stable formulations for stock piling at ambient temperatures [34]. It has been suggested that AuNPs in the range of 8–17 nm induce a strong antibody response with low cytotoxicity [21,35]. Accordingly, we sought to make AuNPs in this size range and investigate their potential use as an antigen carrier for an influenza vaccine.

This study presents the first use of AuNPs as an antigen carrier of M2e. To allow attachment of M2e peptide on the surface of AuNPs through the thiol group, a cysteine was added to the 'C' terminal of M2e (to maintain natural orientation of M2e after conjugation). The consensus human influenza virus M2e sequence contains two cysteines at positions 17 and 19 [7]. To avoid crosslinking and aggregation of AuNPs due to multiple thiol groups in a molecule, the two naturally occurring cysteines were replaced by serines. It has been shown that this substitution does not affect the immunogenicity of M2e [14,36]. Intranasal mucosal vaccination is more convenient than intramuscular vaccination and can offer potential benefits in stimulating mucosal immunity. CpG–oligodeoxynucleotide (ODN), which is a synthetic ODN containing unmethylated CpG motifs, has been extensively used as a mucosal adjuvant that can effectively stimulate Th1-biased cytokines and a high level of IgG2a antibody [37-40]. Therefore, in this study, our goal was to develop a M2e–AuNP conjugate and test its protective ability against influenza A virus in a mouse challenge model, and to determine whether addition of a soluble form of CpG as an adjuvant could further improve the immune response.

Materials & methods

Chemicals

Gold(III) chloride trihydrate (520918-5G), trisodium citratedihydrate (S1804-500G), phosphate–citrate buffer tablet (P4809-50TAB) and gold etchant standard KI and I_2 (651818-500ML) were purchased from Sigma-Aldrich (MO, USA). Sodium chloride (BDH0286-500G) and Tween® 20 (BP337-100), were purchased from Fisher Scientific (PA, USA). *O*-phenylenediamine (OPD; 00–2003) was obtained from Invitrogen (NY, USA). Milli-Q (Millipore, MA, USA) water with a resistance of 18.2 MΩ·cm was used in all the experiments.

Peptides, antibodies & oligonucleotides

M2e (acetylated-SLLTEVETPIRNEWGSRSNDSSDC-amidated; molecular weight: 2736 Da) was chemically synthesized by AAPPTec, LLC, KY, USA. ODN 1826 VacciGrade (CpG ODN, type B murine-TLR9 agonist) was purchased from InvivoGen (CA, USA). Avian Influenza A M2 antibody was obtained from ProSci, Inc. (CA, USA). All other secondary antibodies were purchased from Southern Biotech (AL, USA).

Fabrication & characterization of AuNPs

AuNPs with a diameter of 12 nm were synthesized by the Turkevich method [41,42] of reduction of gold(III) chloride trihydrate ($HAuCl_4 \cdot 3H_2O$) with trisodium citrate dihydrate ($Na_3C_6H_5O_7.2H_2O$). A total of 300 ml of 1-mM gold(III) chloride trihydrate solution was brought to boil under vigorous stirring. Then 30 ml of 40-mM trisodium citrate dehydrate

was added into the boiling solution. After 15 min of reaction the solution turned reddish and the reaction was stopped. Upon completion of reaction, 250 ml of AuNP suspension was obtained due to loss of water during boiling. The size of AuNPs was confirmed by using a transmission electron microscope and dynamic light scattering (DLS). Transmission electron micrographs (TEMs) were obtained on a Hitachi (MI, USA) H-8100 transmission electron microscope. TEM samples were prepared by evaporating one drop of AuNP suspension on a 300 mesh copper grid coated with carbon film. Size distribution was investigated by DLS (Zetatrac, Microtrac Inc., PA, USA). UV-visible (vis) absorbance spectra were recorded at room temperature with Cary 300 UV-vis spectrophotometer (Agilent Technologies, Inc., CA, USA).

Conjugating peptides to AuNPs

Tween 20 (0.1%) was added into AuNP suspension to improve the stability of AuNPs. Then 1 ml (0.0225 nmol/ml) AuNP suspension was centrifuged down at 17,000 *g* for 25 min at 4°C. The pellet containing AuNPs (88 μl) was collected by removing the excess supernatant (912 μl). To achieve M2e conjugation, 12 μl of 1-mM M2e in water (equivalent to 32.8 μg of M2e) was added to 88 μl of the AuNP suspension (0.0225 nmol of AuNPs), resulting in approximately 500 M excess of M2e. The addition was performed dropwise and the mixture was allowed to equilibrate overnight at 4°C to obtain 100 μl of the vaccine formulation. This formulation allowed immunization of four mice (25 μl containing 8.2 μg of M2e per mouse). M2e–AuNP conjugation was confirmed by measuring the shift in absorbance wavelength and the stability of the conjugate was assessed by adding 1% sodium chloride [43]. The stability test also included measurement of the wavelength of the M2e–AuNP conjugate after lyophilization.

X-ray photoelectron spectroscopy of M2e–AuNPs

An x-ray photoelectron spectroscopy (XPS) analysis of M2e–AuNPs was performed using PHI 5000 VersaProbe II Scanning Microprobe with the PHI MultiPak® Version 9.3 software (Physical Electronics Inc., MN, USA). All spectra were acquired with a monochromatic aluminum x-ray source ($h\nu$ = 1486.6 eV), a 100 μm spot size in point mode, both electron and ion neutralization, and a hemispherical analyzer pass energy of 29.35 eV. Samples of bare AuNPs (unconjugated) and M2e–AuNPs were lyophilized and the resulting powder was mounted with double-sided copper tape to the XPS sample holder. M2e–AuNPs were washed five-times with wash–spin cycles to remove unbound M2e before lyophilization. Care was taken to ensure that a sample-covered area with no adhesive visible to the detector was used for all analyses. All spectra were collected at a 45° take-off angle. Spectra were referenced to the Au 4f 7/2 peak energy of 84 eV. The relative atomic concentration was calculated through PHI MultiPak standard sensitivity factors.

Quantification of M2e–AuNPs

The amount of M2e peptide conjugated on the surface of AuNPs was measured by ELISA. The sample used for quantification was prepared as follows: AuNPs (1 ml) were conjugated with excess M2e peptide by overnight incubation at 4°C, and the excess peptide was removed by washing three times in water by repeat wash–spin cycles. The final suspension was prepared in 50 μl of water by removing 950 μl supernatant in the last spin cycle. Gold etching solution comprising of KI and I_2 in phosphate-buffered saline (PBS) was added to etch AuNPs for 15 min, which dissolved AuNPs and released M2e into the solution. M2e standard solution was made by first etching bare AuNPs (without M2e conjugation) to obtain the same background signal as present in the M2e–AuNP etched solution. Next, known amounts of M2e were added into this etched gold solution to prepare standard solutions. ELISA plates were then coated by the standard solutions and the unknown

samples (in triplicate). Plates were blocked with 100 µl of 3% bovine serum albumin in PBS for 2 h at room temperature. Mouse anti-M2e antibody was used as the detection antibody and horseradish peroxidase-labeled goat antimouse antibody was used as the secondary antibody. Color was developed using OPD as the substrate. After plotting a curve of the standard solution, the optical density value of unknown samples was interpolated to calculate the corresponding concentration of M2e in the unknown samples.

Immunization of mice

BALB/c female 6–8-week-old mice were purchased from Charles River Laboratories (MA, USA) and were maintained at Texas Tech University Animal Care Services (TX, USA). All animal treatments were performed according to Texas Tech University Animal Care and Use Committee (IACUC) approved procedures. Two independent immunization studies were performed, each with three to five mice per group. Mice were anesthetized and intranasally administered M2e alone, M2e with soluble adjuvant CpG–ODN, or M2e–AuNP conjugates with or without soluble adjuvant CpG–ODN. The dosage of M2e was 8.2 µg for all groups of mice. To maintain dose consistency, unbound excess M2e was not removed from formulations containing AuNPs. As discussed in the results section, approximately 1.25 µg of the 8.2 µg M2e is bound to AuNPs, while the remaining M2e is present in a soluble form. Each mouse in the M2e–AuNP-vaccinated group received 60 µg of AuNPs, while the adjuvant groups additionally received 20 µg of soluble CpG per mouse. All formulations were administered in a volume of 25 µl water given dropwise to the nares at day 1 and repeated (boosted) at day 21. Blood was collected through retro-orbital sinuses at days 0, 21 and 42. The collected sera were centrifuged at 17,000 × *g* for 15 min and stored at −20°C until analysis.

Antibody measuremen

M2e-specific antibodies generated by immunized mice were measured by ELISA. Ninety-six well plates (MaxiSorp®, Sigma-Aldrich,) were coated overnight at 4°C with 50 µl of 5-µg/ml M2e peptide in PBS. Plates were blocked with 100 µl of 3% bovine serum albumin in PBS for 2 h at room temperature. A total of 50 µl of serum dilution samples were added and incubated for 1 h at room temperature. Plates were incubated with 50 µl of 1:4000 dilution of horseradish peroxidase-labeled anti-IgG, anti-IgG1 or anti-IgG2a secondary antibodies for 1 h at room temperature. Plates were washed three times with 0.05% Tween 20 in PBS between each step using ELx405 microplate washer (BioTek, VT, USA). Color was developed with OPD as the substrate. After 5–10 min, 50 µl of 3% phosphoric acid was added to terminate the reaction. Absorbance at 490 nm was recorded by the SpectraMax Plus384 microplate reader (Molecular Devices, LLC, CA, USA).

Influenza A virus challenge

Mice were anesthetized and intranasally inoculated with 30 µl of influenza A virus (H1N1 – A/PR/8/34) at approximately a 5 × lethal dose 50% (LD_{50}) 3 weeks after boost immunization. Weight loss was recorded daily and mice were monitored for survival for 2 weeks. If mice experienced weight loss of over 25%, they were euthanized and included as the experimental end point.

Statistical analysis

All statistical analyses were performed using GraphPad Prism for Windows, version 5.0 (GraphPad Software, Inc., CA, USA). Comparison of antibody titers between groups of mice was performed with two-way analysis of variance (ANOVA) and a Bonferroni test at a value of $p < 0.05$ for statistical significance. Comparison of survival of influenza-challenged

mice between groups of mice was carried out with log-rank chi-square (Mantel–Cox) test with a value of $p < 0.05$ for statistical significance.

Results & discussion

Gold nanoparticle synthesis

We selected AuNPs as the M2e peptide carrier because AuNPs can be chemically synthesized with tight control over size, low polydispersity, and can be easily conjugated with antigens at a high surface density through the thiol–gold interaction. We further decided to make AuNPs with a diameter between 8 and 17 nm because it is reported to offer higher antigenicity and low cytotoxicity [21,35]. It has been shown that the particle size of AuNPs can be readily controlled by controlling the specific ratio of gold to citrate ion in the reaction mixture. Citrate ion functions as a reducing agent and a capping agent. AuNPs with a diameter of 12 nm were fabricated following the formulation reported in the 'Materials & methods' section. AuNP samples were monitored using TEM and DLS to determine size distribution (Figure 1). As shown in Figure 1A, colloidal gold was well dispersed in solution with a uniform shape and size. The mean AuNP size obtained with DLS was 12 nm (Figure 1B). The size was also verified by TEM imaging and was found to be 13 ± 2 nm.

Conjugation of M2e–AuNPs & their stability

Tween 20 (0.1%) was first added to AuNP suspension prior to addition of M2e peptides to provide a steric shield on gold surfaces, thus improving stability of the suspension and preventing large crosslinked aggregation of AuNPs from centrifugation at high speed [44]. To obtain full coverage of AuNP surfaces, M2e was added in a molar excess. M2e–AuNP conjugates were monitored by scanning the surface plasmon peak using UV-vis spectra. It is well known that the absorbed wavelength will shift as a result of changes in the size of AuNPs [28,45]. Original AuNPs with a mean diameter of 12 nm had an absorption maximum of 518 nm (Figure 2A). After conjugation of M2e peptide, the absorbance wavelength shifted to 521 nm, indicating stable conjugation between M2e and AuNPs. Figure 2A shows that subsequent addition of 20 μg of CpG to M2e–AuNP conjugates did not disturb the stability of the colloidal suspension. The stability of conjugated nanoparticles was also confirmed by the absence of aggregation in the presence of 1% of NaCl [43]; while M2e–AuNP conjugates remained stable, bare AuNPs aggregated immediately in 1% NaCl (Supplementary Figure 1A; see online at www.futuremedicine.com/doi/suppl/10.2217/nnm.13.58). Mucus presents a complex viscoelastic environment with a high salt content that can screen the repulsive electrostatic forces of citrate ions and cause irreversible aggregation of AuNPs. Although we did not directly test the stability of M2e–AuNPs in mucus, we can infer from the stability of AuNPs in 1% NaCl that they should be stable in mucus. Furthermore, the M2e–AuNP conjugates could remain stable after storage at either 4°C or ambient temperature for at least 2 weeks, which was verified by an absence of variation in UV-vis spectra (Supplementary Figure 1B).

To test the stability of M2e–AuNPs as a dry powder, we first lyophilized the formulation then resuspended the lyophilized powder in water and compared the absorbance wavelength with nonlyophilized M2e–AuNP conjugates. The lyophilized M2e–AuNP conjugates were found to easily resuspend in water. The UV-vis spectra curves of lyophilized and non-lyophilized M2e–AuNP conjugates were found to overlap with each other (Figure 2B), with both exhibiting an absorbance maximum at 521 nm. By contrast, as seen in Figure 2B, lyophilized bare AuNPs exhibited aggregation and could not be resuspended. A TEM of AuNPs before and after lyophilization (Figure 2C & D) further confirmed that M2e–AuNPs were uniformly resuspended in water and did not aggregate. At equilibrium, the bond between AuNPs and the thiol of M2e is expected to have a certain dissociation constant.

However, the presence of excess M2e in solution is expected to force a continuous coverage of the AuNP surface. Furthermore, the stability of M2e–AuNP conjugation will be further enhanced if the formulation is stored in a solid state following lyophilization. Taken together, this suggests that M2e stabilizes AuNPs, and M2e–AuNP conjugates have the potential for storage at room temperature, thus offering an advantage in transportation of the formulation across vast geographical distances for distribution to the masses.

XPS spectra of M2e–AuNPs

To further analyze the M2e–AuNP conjugate, we performed an XPS analysis of the lyophilized sample and compared the spectra to lyophilized bare AuNPs (without conjugation). Overall, the relative composition of bare AuNPs was 54.4% gold, 42.0% carbon and 3.6% oxygen. This relative composition was consistent within 1% for various 100-μm spot scans. The overall relative composition of the M2e–AuNP conjugates varied more for different 100-μm spot scans, but were always within the following ranges: 15–25.5% gold, 60–71% carbon, 8.5–10% oxygen, 3–6% nitrogen and undetectable to trace amounts of sulfur. These elements are expected based on the molecular structure of the peptide. Evidence of bonding between the M2e peptide and the gold can be seen in the high-energy shoulder present in both the 7/2 and 5/2 peaks of the Au 4f tight scan spectra of M2e–AuNP, which is absent in the bare AuNP spectra (Figure 3A). Furthermore, the C 1s tight scan shows the expected multiple bonding states for the carbon associated with the M2e–AuNP conjugates versus the simple fortuitous carbon associated with the bare AuNPs (Figure 3B). Additional evidence of M2e conjugation to AuNPs can be seen from the higher normalized intensity of nitrogen from M2e–AuNP conjugates (arising from nitrogen in the M2e peptide), as compared with bare AuNPs, which exhibit low nitrogen association (Figure 3C).

Amount of M2e conjugated to AuNPs

After verifying that M2e was successfully and stably conjugated on AuNPs, we next determined the number of M2e molecules attached on the AuNP surface. The total number of AuNPs in the 250-ml solution was calculated as per the following formula under the assumption that all gold chloride trihydrate reacted completely and that all resulting nanoparticles were of uniform size:

$$Number\ of\ AuNPs\ in\ 250\ ml\ of\ solution = \frac{M_{Au} \times 10^{21}}{(\rho_{Au})\,\frac{4}{3}\pi\left(\frac{d}{2}\right)^3}$$

where M_{Au} is the mass of gold involved in the reducing reaction, which is 0.06 g; ρ_{Au} is the density of gold, which is 19.3 g/ml; and d is the diameter of the AuNPs, which is 12 nm. After calculation, the total number of AuNPs in the 250-ml solution was found to be 3.4×10^{15}. This is also equivalent to 1.36×10^{13} AuNPs/ml or 0.0225 nmol/ml of AuNPs (obtained by dividing 1.36×10^{13} AuNPs/ml by the Avagadro number). Based on quantitative ELISA, we found that when 8.2 μg of M2e is mixed with 250 μl of AuNP suspension, which is equal to 3.4×10^{12} AuNPs, 1.25 ± 0.25 μg of M2e is bound to the AuNP surface, translating into 80 ± 16 molecules of M2e conjugated on each AuNP (assuming uniform coverage of all particles). This number is approximately five-times the amount of M2 (~16) [5,6] and almost equal to the amount of NA molecules (~90) that are naturally found on influenza virions [5,46]. Converting M2e conjugation into percentage mass, it amounts to 2% M2e by mass. Other methods reporting attachment of M2e to different nanoparticles have reported similar levels of M2e attachment. For example, the

study by Song *et al.* showed that M2 formed approximately 1% of the total protein of the virus-like particles [13].

Effect of AuNPs & CpG on immune response towards M2e Serum IgG

It has been shown in numerous studies that M2e is a poor immunogen [47,48]. Thus, we examined the ability of AuNPs and CpG (a known adjuvant) to improve the immunogenicity of M2e. AuNPs were conjugated with M2e to form M2e–AuNP conjugates and were used to immunize mice intranasally with or without addition of soluble CpG as an adjuvant. For comparison, separate groups of mice received M2e peptide alone or M2e peptide with soluble CpG as the adjuvant. To investigate the antibody response of immunized mice, blood was collected on days 21 and 42 postimmunization. An ELISA was performed on pooled sera for each group to obtain a dilution curve of M2e-specific IgG antibodies for day 21 (Figure 4A) and 42 (Figure 4B). Figure 4A & B demonstrates that, as expected, M2e is poorly immunogenic and that addition of soluble CpG to soluble M2e does not result in a significant improvement in anti-M2e serum IgG. This result is consistent with a previous study, which found that for intraperitoneally immunized Balb/c mice, the addition of CpG as an adjuvant to M2e did not result in a significant improvement in IgG titers [40]. However, upon conjugation of M2e to AuNPs an increase in anti-M2e serum IgG levels could be seen. This enhancement was more prominent on day 42 (Figure 4B). Incorporation of soluble CpG into the M2e–AuNP conjugate formulation further dramatically increased the serum anti-M2e IgG levels. Based on the pooled serum curves, we selected a serum dilution of 1:200 to further analyze M2e-specific IgG antibody response for individual mice in each group to assess intergroup variability (Figure 4C). On day 21, M2e–AuNP without CpG did not generate strong anti-M2e IgG antibodies, whereas addition of CpG significantly increased the number of M2e-specific antibodies in sera ($p < 0.001$ analyzed by two-way ANOVA Bonferroni test). On day 42, the M2e–AuNP formulation successfully elicited higher anti-M2e IgG antibodies compared with control groups ($p < 0.01$ analyzed by two-way ANOVA Bonferroni test). The addition of CpG to M2e–AuNP conjugates significantly ($p < 0.001$) enhanced the M2e-specific IgG antibody production further compared with the nonadjuvant group. It is important to note that the interanimal variation with use of CpG in the M2e–AuNP group is low, suggesting a synergistic effect of AuNPs and CpG. The data presented combine results of two independent experiments.

Serum IgG subtypes

It has been generally accepted that Th1-type immune response is more critical for restricting viral infections [49,50]. In other words, higher levels of M2e-specific IgG2a antibodies correlate with viral clearance and protection against influenza challenge. Thus, we examined Th1/Th2 type responses by obtaining the dilution curve of M2e-specific IgG1 (Figure 5A) and IgG2a antibodies (Figure 5B) for day 42, and by measuring M2e-specific IgG1/IgG2a in serum dilution samples (1:200) (Figure 5C). At 42 days postimmunization, the M2e–AuNP formulation induced a skewed immune response with higher IgG1 to IgG2a antibody levels. Addition of soluble CpG to the M2e–AuNP formulation not only improved the M2e-specific IgG1 antibody response ($p < 0.001$) compared with the nonadjuvant group, but also significantly enhanced M2e-specific IgG2a antibody response ($p < 0.001$), resulting in an elevated, yet balanced, IgG1/IgG2a response. Previous studies have shown that CpG motifs predominantly induce antigen-specific IgG2a, that is, a Th1 humoral and cell-mediated response [37-40]. Since the AuNP antigen carrier also participates in the antibody stimulation process with adjuvant CpG–ODN, we suspect that the balanced IgG1/IgG2a antibody response may partly be due to co-administration of AuNPs with CpG–ODN. However, more studies are required to verify this.

In vitro cross-reactivity of antibodies to different influenza strains

Next we examined the potential of the consensus M2e peptide attached to AuNPs as a universal influenza vaccine by assessing the ability of serum IgG to bind to native M2 expressed on the surface of three different influenza strains. Accordingly, Philippines-H3N2, PR8-H1N1 and WSNH1N1 were coated as capture antigens for ELISA to evaluate whether the serum of mice immunized with the consensus M2e–AuNPs could detect native M2 expressed on the envelope of these viruses. With the exception of two cysteine substitutions to replace the serines at positions 17 and 19, the M2e peptide used for immunization matches the native M2 sequence of WSN-H1N1 and Philippines-H3N2. However, PR8-H1N1 has one amino acid change (D to G at position 21) compared with the consensus M2e used for immunization (Figure 6B). It can be seen from Figure 6 that serum IgG from mice immunized with M2e–AuNPs with soluble CpG had strong reactivity against WSN-H1N1 and PR8-H1N1 ($p < 0.001$, analyzed by two-way ANOVA Bonferroni Test) as compared with mice that received M2e–AuNPs without CpG. Interestingly, mouse serum IgG showed a lower reactivity ($p < 0.05$) against the Philippines-H3N2 influenza strain, despite the fact that native M2 present on Philippines-H3N2 has the same sequence as the M2e peptide used for immunization. This suggests that the M2 molecule on Philippines-H3N2 may be poorly accessible to antibodies for attachment and binding to occur.

Protection against live influenza challenge

Results from ELISA demonstrated that attachment of M2e to AuNPs coupled with the use of soluble CpG as an adjuvant significantly enhanced the M2e-specific IgG antibodies and induced a balanced IgG1/IgG2a response in mouse serum. We next investigated the protective potential of this immune response. Mice were challenged using a lethal dose of PR8 influenza virus (~5 × LD_{50}), because the M2 sequence of PR8-H1N1 is different from the M2e sequence used for immunization, we considered it to be a more stringent test of vaccine efficacy compared with challenge with WSN-H1N1 or Philippines-H3N2. It was found that weight loss occurred in all groups, including immunized and the naive groups (Figure 7A). Mice receiving M2e peptide were not protected, and demonstrated weight loss and mortality similar to naive (nonvaccinated) mice, and M2e coformulated with soluble CpG resulted in only a 20% survival rate (one out of five mice survived). Mice receiving M2e–AuNP formulation without CpG as an adjuvant lost weight at a slower rate compared with the control mice (naive, M2e alone and M2e with soluble CpG). Although IgG serum antibody results showed that mice vaccinated with M2e–AuNP without CpG as adjuvant elicited a strong immune response ($p < 0.01$), only partial protection was observed against a live influenza challenge (five out of eight mice survived). Interestingly, mice receiving M2e–AuNP conjugates coformulated with CpG as an adjuvant lost weight sooner, but the drop was less severe compared with other groups of mice. Furthermore, supplementation of the M2e–AuNP conjugates with CpG as an adjuvant resulted in complete protection against PR8 influenza virus challenge (Figure 7B), which correlates with the significantly higher anti-M2e IgG titers as compared with the M2e–AuNP without CpG group. All mice (eight out of eight) vaccinated with M2e–AuNP and soluble CpG as the adjuvant began to recover at days 6–7 postchallenge and survived, whereas all (eight out of eight) naive mice died after day 8 post-virus challenge ($p < 0.01$, analyzed by Log-rank Mantel–Cox test).

It should be noted that inclusion of CpG with the M2e peptide (without AuNPs) could only induce a fairly low level of M2e-specific antibodies and did not significantly improve the survival rate (one out of five survived) as compared with the M2e alone formulation. This result is consistent with a previous study, in which CpG administered with M2e through the intraperitoneal injection resulted in survival of just one out of eight Balb/c mice [40]. By contrast, M2e–AuNPs and M2e–AuNPs with adjuvant CpG induced protective M2e-specific antibodies and improved the survival rate to 62.5 and 100%, respectively (Figure 7B). We can

conclude that in our study the significantly enhanced immune response and complete survival after challenge with lethal PR8 influenza virus was largely because of the presence of M2e in a AuNP-conjugated form. It is likely that the attachment of M2e to AuNPs can alter antigen presentation and, thus, result in a superior immune response compared with when AuNPs are not included in the formulation. In accordance, Hashemi *et al.*, who used another nanoparticle, the T7 bacteriophage, reported that T7–M2e nanoparticles induced an anti-M2e immune response and protected mice from lethal influenza challenge, but the M2e peptide failed [18].

Although AuNPs are capable of firmly attaching M2e peptides and can help in the presentation of the influenza antigen in a particulate form to antigen-presenting cells, the delivery mechanism through the nares is still not clear and further studies are required to investigate the penetration of AuNPs through the nasal route and cellular uptake of AuNPs as an antigen carrier. The AuNP can be traced by autometallography at the ultrastructural level [51]. The biodistribution of AuNPs upon intranasal delivery has not been studied. Various bioavailability and toxicity studies related to AuNPs have been carried out and the conclusions suggest that gold particle size, route of administration and properties of the conjugated molecule can affect its biodistribution and safety profile [52-58]. Thus, it becomes important to specifically study the biodistribution and safety of M2e–AuNPs as a vaccine formulation since this is the first time M2e has been conjugated to AuNPs. To perform biodistribution studies, gold content in different tissues, such as lung and liver, can be readily quantified by inductively coupled plasma mass spectrometry [59]. Based on the ELISA result of binding of serum IgG to native M2 expressed on the surface of influenza A viruses (Philippines-H3N2, PR8-H1N1 and WSN-H1N1), we know that M2e-specific IgG antibody could recognize the native M2 expressed on different virus strains to a great extent. However, further *in vivo* challenge studies with a large panel of different virus subtypes is still required to confirm the effectiveness of M2e–AuNP conjugates as a universal antigen for protecting against different influenza A subtypes.

Conclusion

AuNPs with a diameter of 12 nm were synthesized with uniform shape and size and conjugated with M2e using the gold–thiol interaction. M2e–AuNP conjugates enabled stimulation of M2e-specific IgG antibodies, which could recognize M2e and native M2 on influenza A viruses, and partially protected mice from lethal PR8 influenza A virus challenge. Addition of CpG–ODN as a soluble adjuvant further improved the immune response, providing complete protection against the lethal dose of PR8 virus challenge. Overall, this study demonstrates the potential of using AuNPs as a platform for the development of an influenza vaccine.

Future perspective

In this study, we demonstrated that AuNPs provide a simple way to conjugate M2e peptide using the gold–thiol interaction, and provide a promising platform as an antigen carrier of this poorly immunogenic peptide for immunization against influenza A viruses. The adjuvant function of gold nanoparticles makes them a promising material for future universal influenza vaccine development. Since both AuNPs and M2e can be chemically synthesized, it can potentially allow for a fully synthetic approach for vaccine production. In addition, it can allow for development of new vaccines that can utilize AuNPs as a basal structure to conjugate other synthesized peptides as co-antigens or adjuvants. Successful development of this approach will not only provide a means to develop a universal influenza vaccine, but will also provide a logistical advantage in delivery, since it has potential to be self-administered as nasal drops and does not require trained personnel for administration.

Vaccine delivery through the nasal route has the potential to induce mucosal immunity. Although we did not fully test this potential in our study, we did collect vaginal washes from vaccinated mice and found significant production of anti-M2e IgA in vaginal secretions (Supplementary Figure 2). This suggests that AuNPs could also be used as a platform to develop vaccines against sexually transmitted diseases, such as HIV. Overall, AuNPs offer a promising platform to produce synthetic virus-mimicking structures that could be used to induce systemic and mucosal immune responses against a variety of pathogens.

Executive summary

Synthesis & characterization of M2e–gold nanoparticle conjugate

- Citrate-reduced gold nanoparticles (AuNPs) with a diameter of 12 nm were synthesized and characterized by transmission electron micrography and dynamic light scattering.
- Stable matrix 2 protein (M2e)–AuNP conjugates were made by attaching the M2e peptide to AuNPs through use of the gold–thiol interaction. Stability was confirmed using UV-visible spectroscopy and transmission electron micrography. Further evidence of bonding between M2e peptide with AuNPs was provided using x-ray photoelectron spectroscopy.
- M2e–AuNPs could be lyophilized to be stored as dry powder and were easily resuspended in an aqueous solution demonstrating the potential of perhaps storing the formulation in dry state at room temperatures and reformulating it just prior to use.

Effect of AuNPs & CpG on immune response

- Naive mice and mice vaccinated with M2e alone or with soluble CpG did not induce strong anti-M2e serum IgGs.
- Attachment of M2e to AuNPs improved M2e immunogenicity and vaccinated mice generated M2e-specific serum IgG antibodies.
- Addition of soluble CpG–oligodeoxynucleotide as an adjuvant to M2e–AuNP conjugates significantly increased the anti-M2e IgG antibodies in mice serum compared with no adjuvant group ($p < 0.001$) and stimulated a balanced IgG1/IgG2a response.

Recognition of different influenza viruses & protection against lethal challenge

- The serum from mice immunized with M2e–AuNP conjugate with soluble CpG as adjuvant crossreacted against WSN-H1N1, PR8-H1N1 and Philippines-H3N2.
- While the M2e–AuNP formulation produced only partial protection against lethal influenza virus challenge, addition of CpG as a soluble adjuvant to the conjugates resulted in complete protection against lethal PR8 influenza virus.

Supplementary Material

Refer to Web version on PubMed Central for supplementary material.

Acknowledgments

Research reported in this publication was supported in part by the National Institute of Allergy and Infectious Diseases of the NIH under Award Number R21AI099575.

References

Papers of special note have been highlighted as:

■ of interest

■■ of considerable interest

1. Potter, CW. Chronicle of influenza pandemics. In: Nicholson, KG.; Webster, RG.; Hay, AJ., editors. Textbook of Influenza. Blackwell; Oxford, UK: 1998. p. 3-18.
2. CDC. Estimates of deaths associated with seasonal influenza – United States, 1976–2007. Morb. Mortal. Weekly Rep. 2010; 59(33):1057–1062.
3. Ebrahimi SM, Tebianian M. Influenza A viruses: why focusing on M2e-based universal vaccines. Virus Genes. 2011; 42:1–8. [PubMed: 21082230]
4. Reid AH, Fanning TG, Janczewski TA, McCall S, Taubenberger JK. Characterization of the 1918 “Spanish” influenza virus matrix gene segment. J. Virol. 2002; 76(21):10717–10723. [PubMed: 12368314]
5. Holsinger LJ, Alams R. Influenza virus M2 integral membrane protein is a homotetramer stabilized by formation of disulfide bonds. Virology. 1991; 183(1):32–43. [PubMed: 2053285]
6. Lamb RA, Zebedee SL, Richardson CD. Influenza virus M2 protein is an integral membrane protein expressed on the infected-cell surface. Cell. 1985; 40(3):627. [PubMed: 3882238]
7. Neirynck S, Deroo T, Saelens X, Vanlandschoot P, Jou WM, Fiers W. A universal influenza A vaccine based on the extracellular domain of the M2 protein. Nat. Med. 1999; 5(10):1157–1163. [PubMed: 10502819]
8. Tompkins SM, Zhao ZS, Lo CY, et al. Matrix protein 2 vaccination and protection against influenza viruses, including subtype H5N1. Emer. Infect. Dis. 2007; 13(3):426.
9. Ionescu RM, Przysiecki CT, Liang X, et al. Pharmaceutical and immunological evaluation of human papillomavirus viruslike particle as an antigen carrier. J. Pharm. Sci. 2006; 95(1):70–79. [PubMed: 16315228]
10. Fan J, Liang X, Horton MS, et al. Preclinical study of influenza virus A M2 peptide conjugate vaccines in mice, ferrets, and rhesus monkeys. Vaccine. 2004; 22(23):2993–3003. [PubMed: 15297047]
11. Fu TM, Grimm KM, Citron MP, et al. Comparative immunogenicity evaluations of influenza A virus M2 peptide as recombinant virus like particle or conjugate vaccines in mice and monkeys. Vaccine. 2009; 27(9):1440–1447. [PubMed: 19146898]
12. Ernst WA, Kim HJ, Tumpey TM, et al. Protection against H1, H5, H6 and H9 influenza A infection with liposomal matrix 2 epitope vaccines. Vaccine. 2006; 24(24):5158–5168. [PubMed: 16713037]
13. Song J-M, Wang B-Z, Park K-M, et al. Influenza virus-like particles containing M2 induce broadly cross protective immunity. PLoS One. 2011; 6(1):e14538. [PubMed: 21267073]
14. Huleatt JW, Nakaar V, Desai P, et al. Potent immunogenicity and efficacy of a universal influenza vaccine candidate comprising a recombinant fusion protein linking influenza M2e to the TLR5 ligand flagellin. Vaccine. 2008; 26(2):201–214. [PubMed: 18063235]
15. Kowalczyk W, De La Torre BG, Andreu D. Strategies and limitations in dendrimeric immunogen synthesis. The influenza virus M2e epitope as a case study. Bioconjugate Chem. 2010; 21(1):102–110.
16. Zhao G, Lin Y, Du L, et al. An M2e-based multiple antigenic peptide vaccine protects mice from lethal challenge with divergent H5N1 influenza viruses. Virol. J. 2010; 7(9)
17. De Filette M, Ramne A, Birkett A, et al. The universal influenza vaccine M2e–HBc administered intranasally in combination with the adjuvant CTA1-DD provides complete protection. Vaccine. 2006; 24(5):544–551. [PubMed: 16169634]
18. Hashemi H, Pouyanfard S, Bandehpour M, et al. Immunization with M2e-displaying T7 bacteriophage nanoparticles protects against influenza A virus challenge. PLoS One. 2012; 7(9):e45765. [PubMed: 23029232]

19. De Filette M, Fiers W, Martens W, et al. Improved design and intranasal delivery of an M2e-based human influenza A vaccine. Vaccine. 2006; 24(44-46):6597–6601. [PubMed: 16814430]

20. Gerhard W, Mozdzanowska K, Zharikova D. Prospects for universal influenza virus vaccine. Emerg. Infect. Dis. 2006; 12(4):569–574. [PubMed: 16704803]

21. Chen YS, Hung YC, Lin WH, Huang GS. Assessment of gold nanoparticles as a size-dependent vaccine carrier for enhancing the antibody response against synthetic foot-and-mouth disease virus peptide. Nanotechnology. 2010; 21:195101. [PubMed: 20400818]

■. Demonstrates the effect of gold nanoparticle size on immune response and concludes that 8–17-nm diameter gold nanoparticles are most effective in inducing an immune response against conjugated peptide.

22. Dykman L, Staroverov S, Bogatyrev V, Shchyogolev SY. Adjuvant properties of gold nanoparticles. Nanotech. Russia. 2010; 5(11):748–761.

■■. Systematic review of gold nanoparticles as a vaccine carrier and adjuvant.

23. Cruz LJ, Rueda F, Cordobilla BA, et al. Targeting nanosystems to human DCs via Fc receptor as an effective strategy to deliver antigen for immunotherapy. Mol. Pharm. 2010; 8(1):104–116. [PubMed: 21121669]

24. Hosta-Rigau L, Olmedo I, Arbiol J, Cruz LJ, Kogan MJ, Albericio F. Multifunctionalized gold nanoparticles with peptides targeted to gastrin-releasing peptide receptor of a tumor cell line. Bioconjugate Chem. 2010; 21(6):1070–1078.

25. Vasilenko O, Staroverov S, Yermilov D, Pristensky D, Shchyogolev SY, Dykman L. Obtainment of polyclonal antibodies to clenbuterol with the use of colloidal gold. Immunopharmacol. Immunotoxicol. 2007; 29(3-4):563–568. [PubMed: 18075865]

26. Dykman L, Khlebtsov N. Gold nanoparticles in biomedical applications: recent advances and perspectives. Chem. Soc. Rev. 2012; 41(6):2256–2282. [PubMed: 22130549]

■■. Review of gold nanoparticles for various biomedical applications, including discussion of toxicity and biodistribution.

27. Chithrani BD, Ghazani AA, Chan WCW. Determining the size and shape dependence of gold nanoparticle uptake into mammalian cells. Nano Lett. 2006; 6(4):662–668. [PubMed: 16608261]

28. Jain PK, Lee KS, El-Sayed IH, El-Sayed MA. Calculated absorption and scattering properties of gold nanoparticles of different size, shape, and composition: applications in biological imaging and biomedicine. J. Phys. Chem. B. 2006; 110(14):7238–7248. [PubMed: 16599493]

29. Liu Y, Shipton MK, Ryan J, Kaufman ED, Franzen S, Feldheim DL. Synthesis, stability, and cellular internalization of gold nanoparticles containing mixed peptide-poly (ethylene glycol) monolayers. Anal. Chem. 2007; 79(6):2221–2229. [PubMed: 17288407]

30. Kumar A, Ma H, Zhang X, et al. Gold nanoparticles functionalized with therapeutic and targeted peptides for cancer treatment. Biomaterials. 2012; 33(4):1180–1189. [PubMed: 22056754]

31. Bastús NG, Sánchez-Tilló E, Pujals S, et al. Peptides conjugated to gold nanoparticles induce macrophage activation. Mol. Immunol. 2009; 46(4):743–748. [PubMed: 18996597]

■. Demonstration of the adjuvant property of peptide-conjugated gold nanoparticles through macrophage activation.

32. Duncan B, Kim C, Rotello VM. Gold nanoparticle platforms as drug and biomacromolecule delivery systems. J. Control. Release. 2010; 148(1):122–127. [PubMed: 20547192]

33. Daniel MC, Astruc D. Gold nanoparticles: assembly, supramolecular chemistry, quantum-size-related properties, and applications toward biology, catalysis, and nanotechnology. Chem. Rev. 2004; 104(1):293. [PubMed: 14719978]

34. Lévy R, Thanh NTK, Doty RC, et al. Rational and combinatorial design of peptide capping ligands for gold nanoparticles. J. Am. Chem. Soc. 2004; 126(32):10076–10084. [PubMed: 15303884]

35. Pan Y, Neuss S, Leifert A, et al. Size-dependent cytotoxicity of gold nanoparticles. Small. 2007; 3(11):1941–1949. [PubMed: 17963284]

36. De Filette M, Min Jou W, Birkett A, et al. Universal influenza A vaccine: optimization of M2-based constructs. Virology. 2005; 337(1):149–161. [PubMed: 15914228]

37. Klinman DM. CpG DNA as a vaccine adjuvant. Expert Rev. Vaccines. 2003; 2(2):305–315. [PubMed: 12899580]

38. Millan CLB, Weeratna R, Krieg AM, Siegrist CA, Davis HL. CpG DNA can induce strong Th1 humoral and cell-mediated immune responses against hepatitis B surface antigen in young mice. Proc. Natl Acad. Sci. USA. 1998; 95(26):15553. [PubMed: 9861007]
39. Hayashi M, Satou E, Ueki R, et al. Resistance to influenza A virus infection by antigen-conjugated CpG oligonucleotides, a novel antigen-specific immunomodulator. Biochem. Biophys. Res. Commun. 2005; 329(1):230–236. [PubMed: 15721298]
40. Wu F, Yuan XY, Li J, Chen YH. The co-administration of CpG–ODN influenced protective activity of influenza M2e vaccine. Vaccine. 2009; 27(32):4320–4324. [PubMed: 19410621]

■. CpG-oligodeoxynucleotide is tested as a vaccine adjuvant for influenza M2e vaccine, and the results show that inclusion of CpG does not improve mouse survival compared with M2e alone.

41. Kimling J, Maier M, Okenve B, Kotaidis V, Ballot H, Plech A. Turkevich method for gold nanoparticle synthesis revisited. J. Phys. Chem. B. 2006; 110(32):15700–15707. [PubMed: 16898714]
42. Tkachenko, A.; Xie, H.; Franzen, S.; Feldheim, DL. Assembly and characterization of biomolecule-gold nanoparticle conjugates and their use in intracellular imaging. In: Rosenthal, SJ.; Wright, DW., editors. Nanobiotechnology Protocols. Humana Press; NY, USA: 2005. p. 85-99.

■■. Detailed protocols of conjugating and characterizing biofunctional gold nanoparticles.

43. Lou S, Ye J-Y, Li K-Q, Wu A. A gold nanoparticle-based immunochromatographic assay: the influence of nanoparticulate size. Analyst. 2012; 137(5):1174–1181. [PubMed: 22193208]
44. Duy J, Connell LB, Eck W, Collins SD, Smith RL. Preparation of surfactant-stabilized gold nanoparticle–peptide nucleic acid conjugates. J. Nanoparticle. Res. 2010; 12(7):2363–2369.
45. Link S, El-Sayed MA. Size and temperature dependence of the plasmon absorption of colloidal gold nanoparticles. J. Phys. Chem. B. 1999; 103(21):4212–4217.
46. Amano H, Hosaka Y. Morphological estimation of total number of influenza A type virion spikes. J. Electron Microscopy. 1992; 41(2):104–106.
47. De Filette M, Martens W, Smet A, et al. Universal influenza A M2e–HBc vaccine protects against disease even in the presence of pre-existing anti-HBc antibodies. Vaccine. 2008; 26(51):6503–6507. [PubMed: 18835315]
48. Li K, Luo J, Wang C, He H. α-galactosylceramide potently augments M2e-induced protective immunity against highly pathogenic H5N1 avian influenza virus infection in mice. Vaccine. 2011; 29(44):7711–7717. [PubMed: 21839133]
49. Coutelier JP, Van Der Logt J, Heessen F, Warnier G, Van Snick J. IgG2a restriction of murine antibodies elicited by viral infections. J. Exp. Med. 1987; 165(1):64–69. [PubMed: 3794607]
50. Huber VC, Mckeon RM, Brackin MN, et al. Distinct contributions of vaccine-induced immunoglobulin G1 (IgG1) and IgG2a antibodies to protective immunity against influenza. Clin. Vaccine Immunol. 2006; 13(9):981–990. [PubMed: 16960108]

■. Provides details regarding separate roles of IgG subtypes in vaccination against influenza and suggests the importance of increased IgG1 and IgG2a immune responses for improved protection.

51. Danscher G, Nørgaard JOR. Ultrastructural autometallography: a method for silver amplification of catalytic metals. J. Histochem. Cytochem. 1985; 33(7):706–710. [PubMed: 4008918]
52. Chen Y-S, Hung Y-C, Liau I, Huang G. assessment of the *in vivo* toxicity of gold nanoparticles. Nanoscale Res. Lett. 2009; 4(8):858–864. [PubMed: 20596373]
53. Cho W-S, Cho M, Jeong J, et al. Acute toxicity and pharmacokinetics of 13 nm-sized PEG-coated gold nanoparticles. Toxicol. Appl. Pharmacol. 2009; 236(1):16–24. [PubMed: 19162059]
54. Khlebtsov N, Dykman L. Biodistribution and toxicity of engineered gold nanoparticles: a review of *in vitro* and *in vivo* studies. Chem. Soc. Rev. 2011; 40(3):1647–1671. [PubMed: 21082078]
55. Lasagna-Reeves C, Gonzalez-Romero D, Barria MA, et al. Bioaccumulation and toxicity of gold nanoparticles after repeated administration in mice. Biochem. Biophys. Res. Comm. 2010; 393(4): 649–655. [PubMed: 20153731]
56. Murphy CJ, Gole AM, Stone JW, et al. Gold nanoparticles in biology: beyond toxicity to cellular imaging. Accounts Chem. Res. 2008; 41(12):1721–1730.

57. Paciotti GF, Myer L, Weinreich D, et al. colloidal gold: a novel nanoparticle vector for tumor directed drug delivery. Drug Delivery. 2004; 11(3):169–183. [PubMed: 15204636]

58. Sonavane G, Tomoda K, Makino K. Biodistribution of colloidal gold nanoparticles after intravenous administration: effect of particle size. Colloids Surf. B Biointerfaces. 2008; 66(2): 274–280. [PubMed: 18722754]

59. Allabashi R, Stach W, De La Escosura-Muñiz A, Liste-Calleja L, Merkoçi A. ICP-MS: a powerful technique for quantitative determination of gold nanoparticles without previous dissolving. J. Nanoparticle Res. 2009; 11(8):2003–2011.

■ Website

101. WHO. Influenza (seasonal). 2011. www.who.int/mediacentre/factsheets/fs211/en/index.html

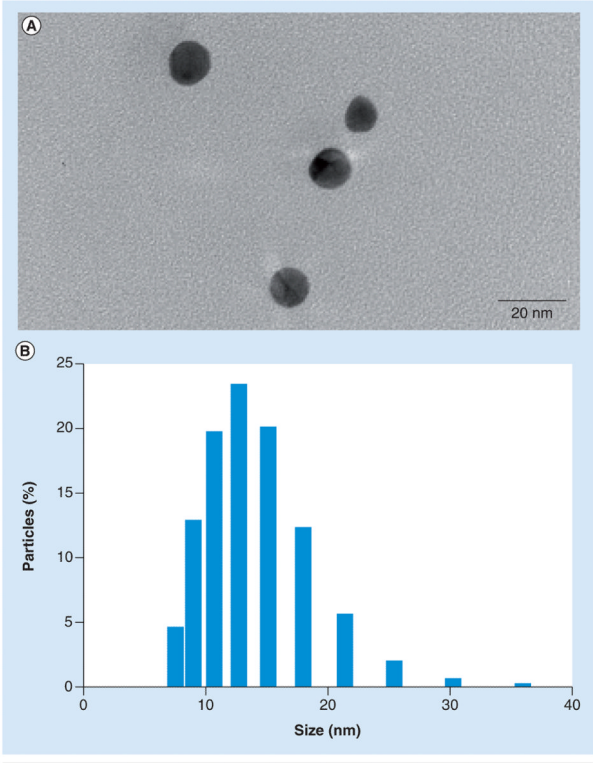

Figure 1. Morphology and size distribution of gold nanoparticles.
(A) Transmission electron micrograph and **(B)** dynamic light scattering data showing size distribution.

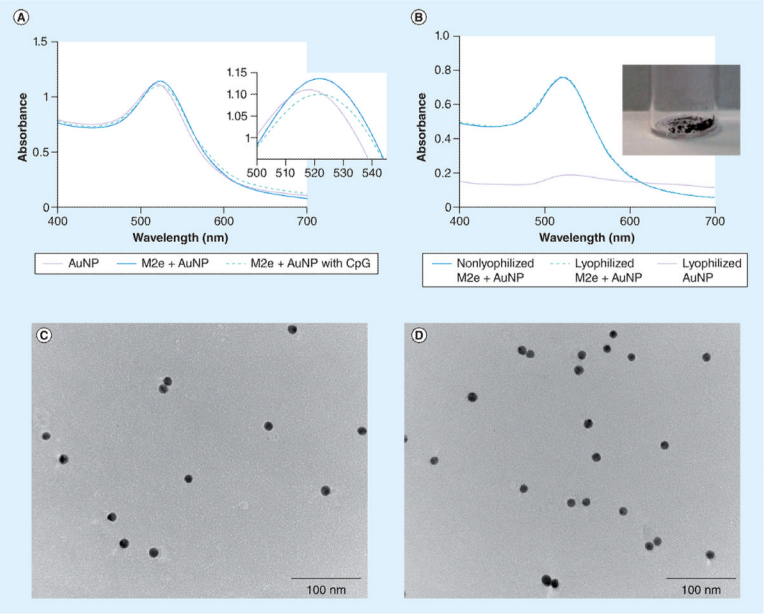

Figure 2. Characterization of gold nanoparticles.

(A) Absorption spectrum of AuNPs before and after conjugation of M2e, and after addition of soluble CpG. Inset shows a close-up of absorption peaks. **(B)** Absorption spectrum of nonlyophilized AuNPs, lyophilized unconjugated AuNPs or lyophilized M2e–AuNP conjugates after resuspension in water. Inset shows a photograph of lyophilized M2e–AuNP conjugates. **(C)** Transmission electron micrograph of nonlyophilized M2e–AuNP conjugates. **(D)** Transmission electron micrograph of a resuspension of lyophilized M2e–AuNP conjugates.

AuNP: Gold nanoparticle.

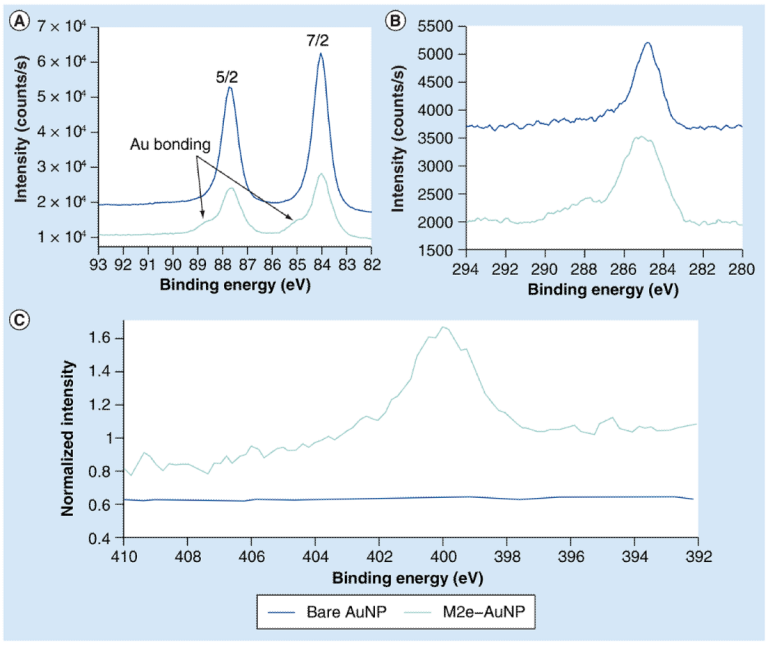

Figure 3. X-ray photoelectron spectroscopy spectra of M2e-conjugated and unconjugated gold nanoparticles.

(A) Tight scan spectra of Au 4f region. Arrows point to the high-energy shoulders. **(B)** Tight scan spectra of C 1s region. **(C)** Tight scan spectra of N 1s region.

AuNP: Gold nanoparticle.

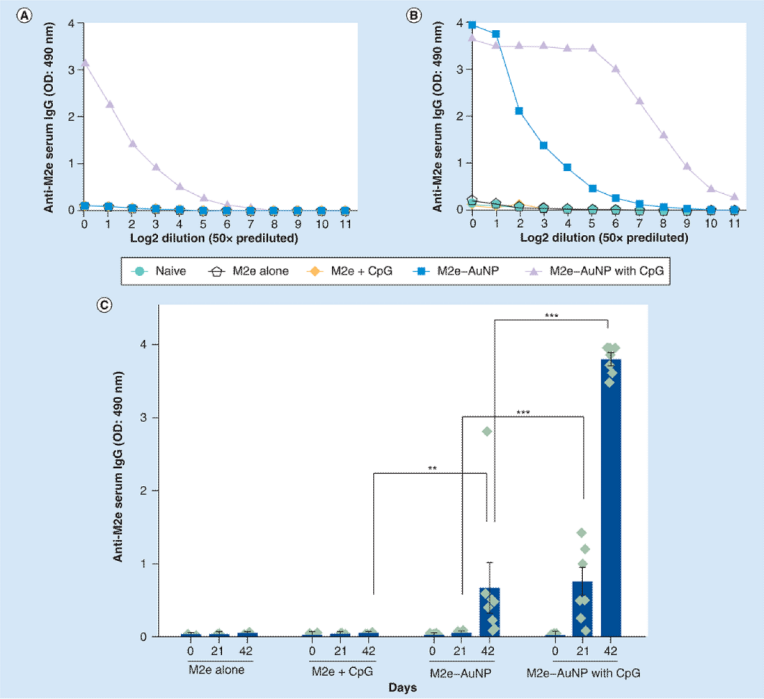

Figure 4. M2e-specific IgG antibody response in mouse serum.

(A) Titration curve for pooled day 21 serum. **(B)** Titration curve for pooled day 42 serum. **(C)** M2e-specific IgG antibodies in 1:200 diluted serum of individual mice of a group. OD measured at 490 nm wavelength. Each diamond in **(C)** represents an animal in a group (n = 3 in M2e alone group, n = 5 in M2e + CpG group and n = 8 for the remainder of the groups), the vertical column represents the mean, and error bars represent standard error of the mean. The data presented combine results of two independent experiments.

**p < 0.01; ***p < 0.001.

AuNP: Gold nanoparticle; OD: Optical density.

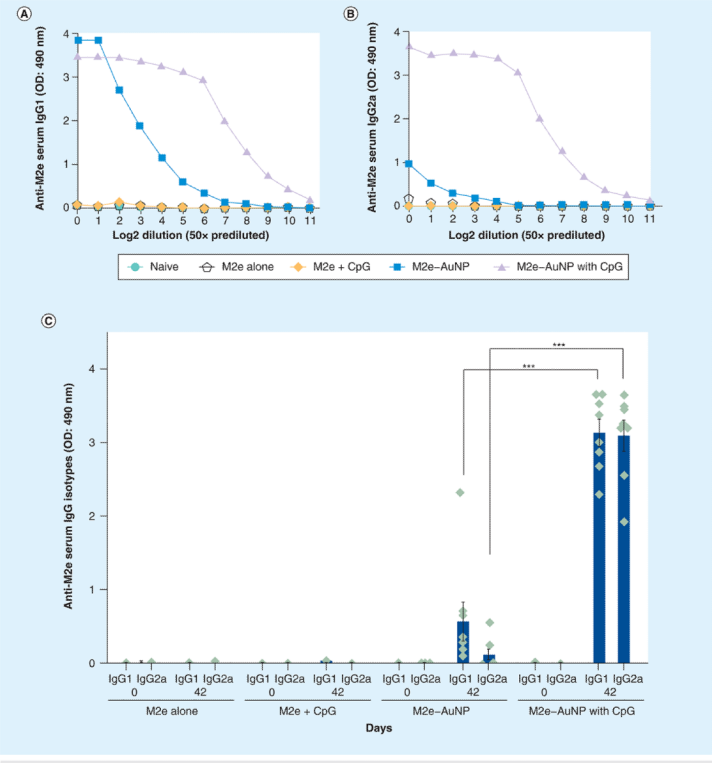

Figure 5. M2e-specific IgG subtypes in mouse serum.

(A) Titration curve for IgG1 in pooled day 42 serum. **(B)** Titration curve for IgG2a in pooled day 42 serum. **(C)** IgG1 and IgG2a antibodies in 1:200 diluted serum of individual mice of a group. OD measured at 490 nm wavelength. Each diamond in **(C)** represents an animal in a group (n = 3 in M2e alone group, n = 5 in M2e + CpG group and n = 8 for the remainder of the groups), the vertical column represents the mean, and error bars represent standard error of the mean. The data presented combine results of two independent experiments.

***$p < 0.001$.

AuNP: Gold nanoparticle; OD: Optical density.

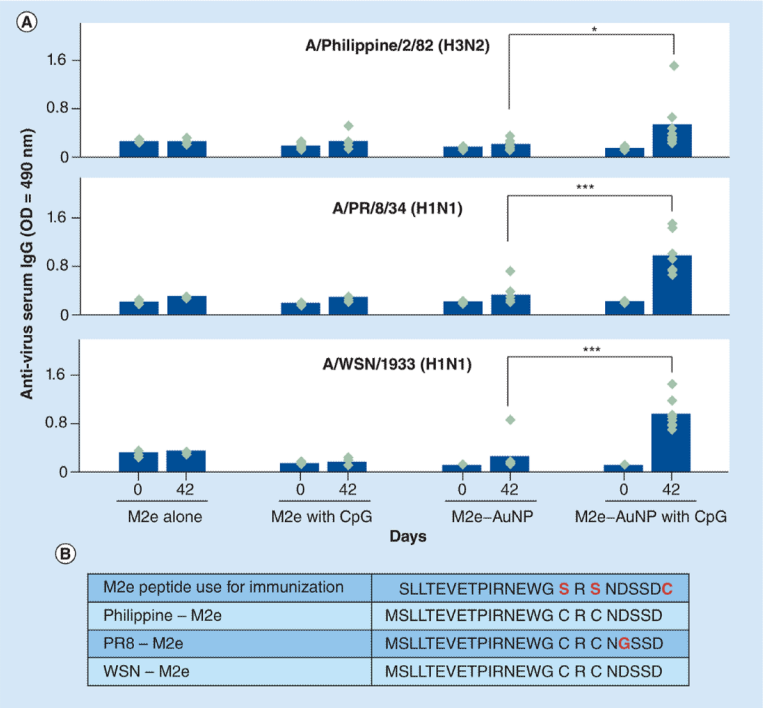

M2e peptide use for immunization	SLLTEVETPIRNEWG S R S NDSSDC
Philippine – M2e	MSLLTEVETPIRNEWG C R C NDSSD
PR8 – M2e	MSLLTEVETPIRNEWG C R C NGSSD
WSN – M2e	MSLLTEVETPIRNEWG C R C NDSSD

Figure 6. Cross-reactivity of mouse serum IgG (1:50 dilution) against native M2 expressed on three influenza A viruses.

(A) OD measured at 490 nm wavelength. Each diamond represents an animal in a group (n = 3 in M2e alone group, n = 5 in M2e + CpG group and n = 8 for the remainder of the groups). The vertical column represents the mean. **(B)** The table provides sequences of the consensus M2e used for immunization and M2e present on the surface of the three influenza A viruses used in the cross-reactivity ELISA assay (Philippines-H3N2, PR8-H1N1 and WSN-H1N1). The data presented combine results of two independent experiments.

*$p < 0.05$; ***$p < 0.001$.

AuNP: Gold nanoparticle; OD: Optical density.

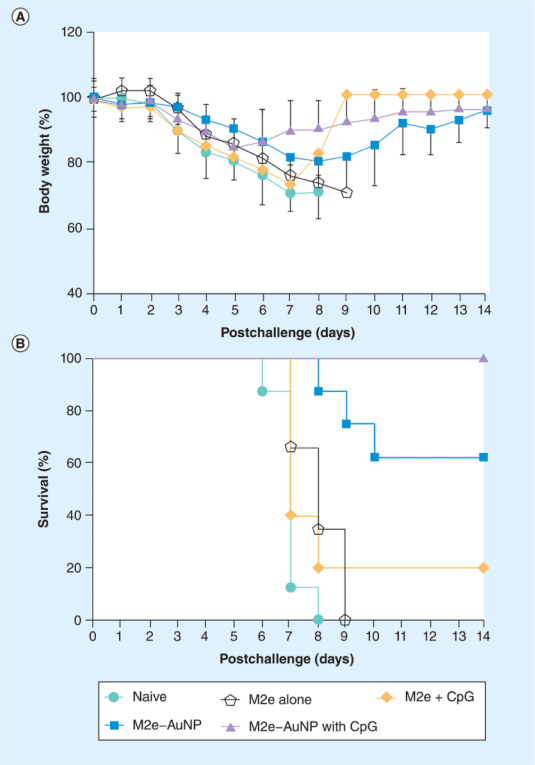

Figure 7. Response of mice to a lethal dose (5 × lethal dose 50%) of influenza PR8 virus.
(A) Weight loss of mice after challenge. **(B)** Survival of mice after challenge. The data presented combine results of two independent experiments (n = 3 in M2e alone group, n = 5 in M2e + CpG group and n = 8 for the remainder of the groups).
AuNP: Gold nanoparticle.